J. Membrane Biol. 58, 81–100 (1981)

The Journal of
Membrane Biology

Topical Review

The Headgroup Conformation of Phospholipids in Membranes

Georg Büldt and Roland Wohlgemuth*

Department of Biophysical Chemistry, Biocenter of the University of Basel, Klingelbergstrasse 70, CH-4056 Basel, Switzerland

I. Features of Lipid Headgroup Conformation and Function

An important feature which determines the physical state of biological membranes is the great variety of individual lipids occurring in different amounts in the composition of the lipid matrices. One may assume that by this means nature has created conditions which optimize the function of the individual highly specialized protein systems in the membranes of different cells and organelles. Present membrane research is far away from presenting an unambiguous proof for this suggestion. Nevertheless for several reconstituted membrane systems, where one integral membrane protein was embedded in one or more kinds of lipids, it was demonstrated that changes in the spectrum of the hydrocarbon chain conformations and their rates of segmental motions (which determine the fluidity of the bilayer) induces variations in the distribution of the proteins in the plane of the membrane and in their function. Large changes in these properties occur for most phospholipids in bilayers during a first-order phase transition between a so-called gel state and a liquid crystalline state. One clear example for the influence of the lipid state on a protein distribution in the bilayer was given by Kleemann and McConnell (1976) in the reconstitution of Ca-ATPase in bilayers of dimyristoyllecithin. Electron micrographs showed the proteins aggregated in the gel state and more randomly distributed in the liquid crystalline state. Considering lipid influence on membrane protein function, the work of Overath, Schairer and Stoffel (1970) gives an example of the way in which the lipid state influences sugar transport through membranes of *Escherichia coli* which were enriched in some lipid species. These examples illustrate the influence of the chain conformation on membrane proteins.

The importance of the headgroup structure is seen in the variation of phospholipid headgroup composition in different systems (Rouser, Nelson, Fleischer & Simon, 1968) and in a specific lipid requirement of some membrane proteins (Sandermann, 1978). In addition, as shown by Träuble and Eibl (1974) using the individual electrostatic properties of some phospholipid headgroups, it is possible to trigger the gel to liquid crystalline phase transition by a change in pH or in the concentration of monovalent and divalent cations or polyelectrolytes (Sackmann, 1978). It is also possible that lipid head groups establish a specific water structure which is used by some proteins for their normal function. So far, however, no experiment has given a detailed picture of the changes in headgroup conformation connected with these processes. On the contrary, experimentalists have only recently established a basis for such investigations through studies on the headgroup conformations of various phospholipids in pure bilayer model membrane systems, with some extensions to natural systems enriched in a specific kind of lipid. The aim of this paper is to summarize in detail the considerable work which has been concerned with headgroup conformation. No discussion will be given of the headgroup interactions with ions and other molecules in the interfacial region, since no firm conformational information on the changes in the lipid headgroup region due to these interactions is as yet available. A presentation of the experimental work of this field can be found in a recent review article of Hauser and Phillips (1979).

In Fig. 1 we have summarized the chemical formulas and nomenclature of the phospholipids which are analyzed in more detail, namely, phosphatidylcholine (PC), phosphatidylethanolamine (PE), phosphatidylglycerol (PG) and phosphatidylserine (PS). A certain chainlength of these phospholipids will be characterized by the usual abbreviation, e.g. DPPC is used for 1,2-dipalmitoyl-*sn*-glycero-3-phosphocholine.

* *Present address:* University of California, Laboratory of Chemical Biodynamics, Berkeley, California 94720.

0022-2631/81/0058-0081 $04.00
© 1981 Springer-Verlag New York Inc.

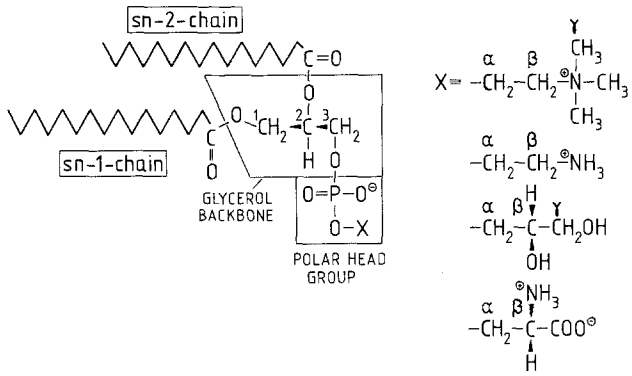

Fig. 1. Chemical structure of a series of phospholipids carrying four different head groups. These lipids (from top to bottom) are PC, PE, PG and PS. The nomenclature of the individual carbon atoms in the polar region is indicated. As depicted in this Figure, naturally occurring phospholipids have the *L* configuration of the C2 carbon atom in the glycerol backbone. The Cβ carbon atom in the head group has the D form in PG and the L form in PS. (For a further discussion of the notation of optically active phospholipids *see* IUPAC-IUB recommendation, *Proc. Nat. Acad. Sci. USA* (1977) **74**:2222-2230)

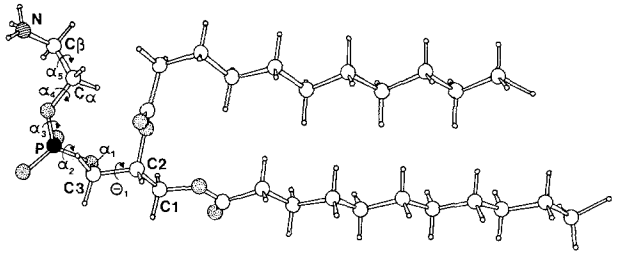

Fig. 2. The conformation of the DLPE molecule as seen in the single-crystal analysis viewed along the crystallographic *c* axis. (Hitchcock et al., 1974; Elder et al., 1977). The nomenclature of the individual carbon atoms used in the text is indicated. According to Sundaralingam (1972) the torsion angle around bond *j* is measured from the *cis*-planar conformation of the $j+1$ and $j-1$ bonds

As a starting point for our discussion we have chosen the single crystal data. Because of the difficulty in growing single crystals of phospholipids suitable for X-ray crystallography, it is only recently that progress in this area has been made. Hitchcock, Mason, Thomas and Shipley (1974) have grown single crystals of *rac*-1,2-dilauroyl-*sn*-glycero-3-phosphoethanolamine (*rac*-DLPE) from acetic acid and determined the molecular conformation of a 1:1-complex with acetic acid by diffraction analysis, which was refined later by Elder, Hitchcock, Mason and Shipley (1977). Recently, Pearson and Pascher (1979) have crystallized 1,2-dimyristoyl-*sn*-glycero-3-phosphocholine (DMPC) with two molecules of water per lipid and solved the molecular structure of this lecithin species. As a representative example we have plotted a DLPE molecule according to these structural data in Fig. 2, also showing the nomenclature of the carbon atoms, which is used for designating the various deuterated segments for the ^{2}H NMR and neutron experiments.

II. How Orientational and Positional Information is Obtained

A. Deuterium Magnetic Resonance

As compared with ^{1}H NMR, the advantage of deuterium magnetic resonance (^{2}H NMR) for studying biological membranes originates from the measurement of the so-called deuterium quadrupole splittings from *selectively deuterated* lipid molecules. These signals can be uniquely connected to local properties like orientation and motion in a lipid molecule. The nuclear spin quantum number of deuterium is $I=1$ while that of hydrogen is $I=1/2$. Nuclei with spin number $I \geqq 1$ have the important property of possessing a nuclear quadrupole moment, which is connected with the spatial orientation of the spin in an external magnetic field H_o. The quadrupole moment gives a measure of the lack of spherical symmetry in the distribution of the electric charges inside the nucleus. This charge distribution can interact with the inhomogeneous electric field produced by the C-D bond electrons. The interaction energy E_Q depends on the direction of the nuclear spin, which determines the orientation of the quadrupole tensor with respect to the axes of symmetry of the local electric field. The orientation of these axes of symmetry as well as the degree of field inhomogeneity are described by the electric field gradient tensor (EFG tensor). For C-D bonds this tensor is axially symmetric around the bond axis, which is the direction of the maximum field gradient. Thus, for a given angle θ of the EFG tensor with respect to the external magnetic field, the interaction energy E_Q for the spin orientations $m=\pm 1$ is different to that for the case when $m=0$, as shown in Fig. 3. Now for another orientation of the C-D bond axis (EFG tensor), each of the two possible E_Q values is changed, thus

$$E_Q(m=\pm 1) = +\tfrac{1}{4} e^2 qQ \cdot \tfrac{1}{2}(3\cos^2\theta - 1) \quad (1)$$

and

$$E_Q(m=0) = -\tfrac{1}{2} e^2 qQ \cdot \tfrac{1}{2}(3\cos^2\theta - 1) \quad (2)$$

where $(e^2 qQ/h)$ is the static quadrupole coupling constant. The difference $\Delta\nu_Q = \Delta E_Q/h$ between these two interaction energies is measured in a ^{2}H NMR experiment from the absorption lines due to the allowed transitions $\Delta m = \pm 1$ between the energy levels $E_m + E_Q$ (where the E_m are the usual Zeeman

energies)

$$\Delta\nu_Q = \frac{3}{2}\frac{e^2qQ}{h}P_2(\theta) \tag{3}$$

with

$$P_2(\theta) = \tfrac{1}{2}(3\cos^2\theta - 1). \tag{4}$$

$\Delta\nu_Q$ is the quadrupole splitting for a fixed C-D orientation which can be observed in a single crystal. The possible range of $\Delta\nu_Q$ can be calculated from Eq. (3) to be 255 kHz for a C-D bond parallel to H_o and -127.5 kHz for a perpendicular orientation, using the static quadrupole coupling constant of 170 kHz (Burnett & Müller, 1971).

In biological membranes, lipid molecules are not fixed in space, but perform different kinds of motions. Rotational motions must take place in a time shorter than the inverse of the quadrupole coupling constant (^{2}H NMR time scale) in order to lead to an averaging of the EFG tensor with respect to these motional axes. Since the lipid molecules in a membrane tend to align each other parallel to the long molecular axis, rotations about this axis (rotator motions) occur with high frequencies (10^7 to 10^{10} Hz) while perpendicular to the axis rapid oscillations with small angular amplitude are still possible. Therefore, for a small domain in a bilayer the orientations of the long axes of the lipids are in fact distributed in a small angular range. In this domain the director axis n is defined as the most *probable direction* of the long axis and coincides in the liquid crystalline phase with the normal to the bilayer surface. It is clear that these motions produce an EFG tensor axially symmetric around this director axis. Therefore, in membranes the orientation of the C-D bond is determined relative to this particular axis n of the small domain by the angle θ. The angle between the director and the magnetic field H_o is given by β (Fig. 3). The quadrupole splitting of such a small domain or of a large oriented monodomain sample is given by

$$\Delta\nu_Q = \frac{3}{2}\frac{e^2qQ}{h}S_{CD}\frac{1}{2}(3\cos^2\beta - 1) \tag{5}$$

with

$$S_{CD} = \overline{P_2(\theta)} = \tfrac{1}{2}(\overline{3\cos^2\theta} - 1), \tag{6}$$

where the average of $\cos^2\theta$ accounts for the above-mentioned overall motions and additional rapid internal motions. This average, however, leads to some difficulties in interpreting S_{CD} order parameters. A measured S_{CD} value can reflect a fairly rigid conformation with only small angular fluctuations about a mean orientation or S_{CD} can mainly be determined by large fluctuations, suggesting a high degree of flexibility.

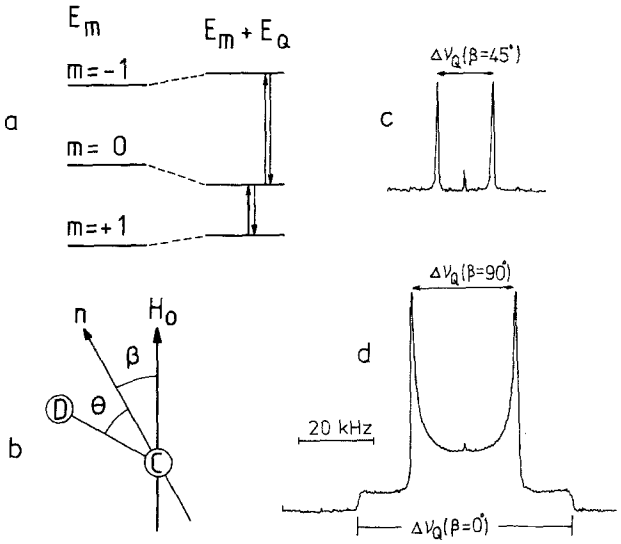

Fig. 3. (*a*) The energy levels for a spin $I=1$ system with and without quadrupole interactions. The changes in the energy levels due to the quadrupole interaction E_Q are largely increased in this drawing. (*b*) The definitions of the angles θ and β. The C-D bond direction has an angle θ with respect to the director n, which, in turn has an angle β with the external magnetic field H_o. (*c*) The experimentally observed absorption spectra, due to transitions of $\Delta m = \pm 1$, for an oriented sample. (*d*) Typical ^{2}H NMR spectrum of randomly oriented multilayers (powder type sample), consisting of a superposition of the quadrupole splittings due to all orientations β

If, on the other hand, there exist sufficient long-lived conformations on the ^{2}H NMR time scale, different quadrupole splittings for the same C-D bond will be seen. In practice, often both hydrogens of the methylene group are substituted resulting in two C-D bonds in the segment. If then two quadrupole splittings are observed, this can be due to the fact that both C-D bonds are not motionally equivalent or that the splittings correspond to two long-lived conformations. In these cases, only by stereospecific introduction of one deuterium in a methylene segment, the quadrupole splittings can be unambiguously assigned. However, up to now, different long-lived conformations for the same segment have not been observed in the liquid crystalline state of the bilayer.

If a rapid isotropic motion of the C-D bond occurs, the EFG tensor is spherically averaged to zero and instead of a quadrupole splitting, a single resonance line is observed. This is seen in the case of small vesicles where the EFG tensor is isotropically averaged due to the tumbling motion of the vesicle and the lateral diffusion of lipids in the bilayer (Stockton, Polnaszek, Tulloch, Hasan & Smith, 1976).

A more extensive discussion of the method of ^2H NMR with respect to lipid membranes has been given by Seelig (1977). With the innovation of the quadrupole echo technique (Davis, Jeffrey, Bloom, Valic & Higgs, 1976), it is possible now to observe the broad ^2H NMR powder spectra in the gel state (Davis, 1979).

B. Phosphorus-31 Nuclear Magnetic Resonance

^{31}P is the only naturally occurring isotope of phosphorus. It has a spin quantum number $I=1/2$ and a relative sensitivity of 0.06 compared to that of ^1H. The physical basis of ^{31}P NMR as applied to phospholipid membranes may be explained as follows: The magnetic field experienced by the phosphorus nucleus is that of the external magnetic field reduced by the field of the bonding electrons (chemical shielding). Experimentally accessible is the chemical shift which corresponds to a chemical shielding relative to a reference compound. Since the electron density is not isotropic but depends on the bonding pattern, the chemical shift becomes a tensorial property analogous to the EFG tensor in ^2H NMR.

Let us start with the assumption that the phospholipid molecule is fixed in a single-crystal lattice. Unlike the EFG tensor of a C-D bond, the chemical shift tensor of the phosphodiester part is not axially symmetric in this lattice. The geometrical information to be obtained is the orientation between the spin and the shift tensor. The z-component of the spin is aligned parallel to the external field. The tensor is connected to the phosphate segment in the lattice. Thus, by orienting the lattice with respect to the magnetic field, it is possible to determine both the orientation and magnitude of the principal tensor elements which describe the *static chemical shift tensor*. These experiments have been performed with a single crystal of bariumdiethylphosphate (BDEP) (Herzfeld, Griffin & Haberkorn, 1978). Their results derived from the BDEP crystal are illustrated in Fig. 4. With powders of various phospholipid classes in a lamellar crystalline phase, the magnitude of the elements of the chemical shift tensor have been found to be in close agreement with the results of BDEP (Kohler & Klein, 1977; Herzfeld et al., 1978; Seelig, 1978). It is important to notice that additional water molecules do not influence the static chemical shift tensor, as has been proved from ^{31}P NMR experiments of fully hydrated DPPC and DPPE bilayers at $-110\,°C$ (Herzfeld et al., 1978).

Bilayer phases will now be considered, where different kinds of anisotropic reorientational motions occur. If these motions are rapid compared to the ^{31}P time scale, the static chemical shift tensor is

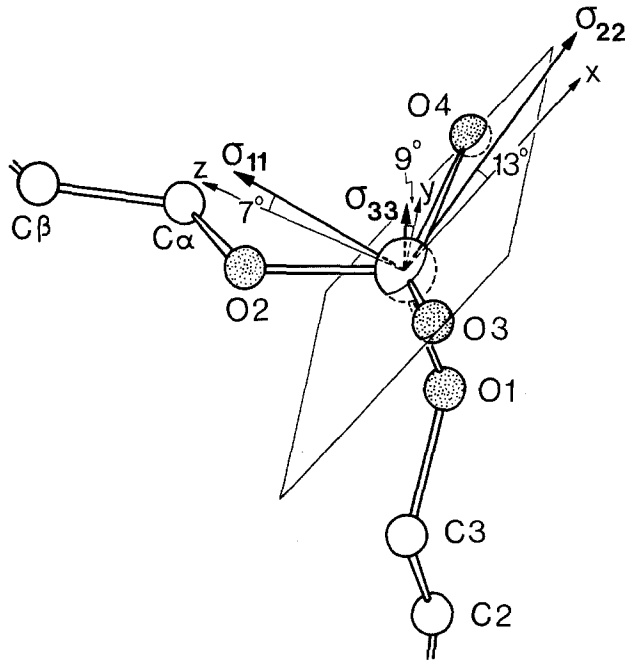

Fig. 4. The orientation of the ^{31}P chemical shift tensor (principal components σ_{ii}) in the molecular frame of the phosphate segment according to the results of a single-crystal study on bariumdiethylphosphate (Herzfeld et al., 1978). The carbon atoms adjacent to the phosphodiester part are designated as in Fig. 2 O3 and O4 are the nonesterified oxygens which together with the phosphate atom define the x–y plane. O1 and O2 connect the phosphate group with the glycerol backbone and the headgroup residue, respectively

partially averaged out. Especially the rotator motion produces an axially symmetric shift tensor. Therefore, as demonstrated in Fig. 5*a* for the case of DPPE, depending on the orientation of the director axis with respect to the magnetic field (indicated by the angle β) the resonance frequency varies between $\sigma_\parallel$ for $\beta=0°$ (magnetic field parallel to the bilayer normal) and $\sigma_\perp$ for $\beta=90°$ (magnetic field perpendicular to the bilayer normal (Seelig & Gally, 1976). *The chemical shift anisotropy* $\Delta\sigma$ is defined as the difference between these two extreme values

$$\Delta\sigma=\sigma_\parallel-\sigma_\perp. \tag{7}$$

As seen in Fig. 5, $\Delta\sigma$ can also be obtained from the spectrum given by a randomly oriented multilamellar sample. This spectrum is, in principle, the superposition of the spectra for all orientations. The quantitative relation between the chemical shift anisotropy and the static chemical shift tensor is given by (Seelig, 1978)

$$\Delta\sigma=S_{11}(\sigma_{11}-\sigma_{22})+S_{33}(\sigma_{33}-\sigma_{22}) \tag{8}$$

where σ_{11}, σ_{22} and σ_{33} are the principal elements of the static shift tensor, S_{11} is the order parameter of the axis connecting the esterified oxygens of the

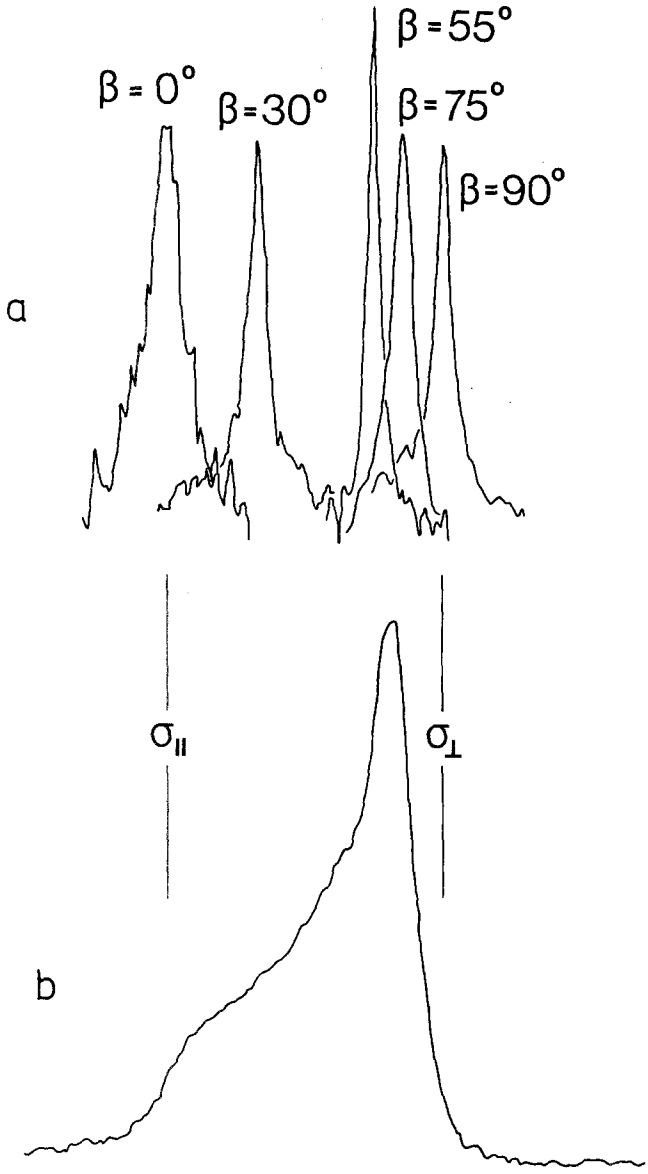

Fig. 5 (*a*) Examples of proton-decoupled ^{31}P NMR spectra (36.5 MHz) of planar oriented multilayers of 1,2-dipalmitoyl-*sn*-glycero-3-phosphoethanolamine (temperature 77 °C; pH 5.5). β is the angle between the magnetic field and the normal to the plane of the membranes. The amplitudes of the individual orientations are not scaled with respect to each other. (*b*) The corresponding spectrum of a randomly oriented multilamellar sample (powder spectrum), which consists of a superposition of spectra with all kinds of orientations

phosphate group, and S_{33} refers to the connecting axis of the nonesterified oxygens (*see* Fig. 4).

The foregoing remarks refer to the bilayer arrangement of hydrated lipids. If other phases like, e.g., hexagonal or micellar phases are considered, characteristic additional motions of the lipids influence the ^{31}P NMR spectra, thereby opening up the opportunity to distinguish different forms of lipid aggregation (Seelig, 1978; Cullis & de Kruijff, 1979).

C. Infrared Spectroscopy

The nuclear motion of a molecular system consisting of N atoms is in general described by $3N$-6 fundamental vibrations. Each may be approximated by a normal vibration (normal mode), that is, by a linear combination of $3N$-6 internal coordinates (stretching, bending torsion) of the same frequency $\tilde{\nu}_i$. This linear combination of synchronous atomic displacements associated to $\tilde{\nu}_i$ is referred to as normal coordinate q_i. Furthermore, the interaction of a normal vibration $\tilde{\nu}_i$ with the infrared radiation field depends on the quantity $(\delta\vec{M}/\delta q_i)_o$, $i=1,2,\ldots,3N-6$. The vector $(\delta\vec{M}/\delta q_i)_o$, represents the derivation of the molecular electric dipole moment $\vec{M}$ with respect to the normal coordinate q_i. It is called "transition dipole moment" or "oscillating dipole moment", and is related to the integrated absorption coefficient $A=\int_0^\infty \varepsilon(\tilde{\nu})\,d\tilde{\nu}$ ($\varepsilon(\tilde{\nu})$ = molar absorption coefficient) of the corresponding infrared band by

$$A_i \propto \nu_i(\vec{E}_o,(\partial\vec{M}/\partial q_i)_o)^2$$
$$= \nu_i E_o^2\,|(\partial\vec{M}/\partial q_i)_o|^2\cos^2(\vec{E}_o,(\partial\vec{M}/\partial q_i)_o). \quad (9)$$

The vector $\vec{E}_o$ denotes the amplitude of the electric field strength acting on the molecule. The last term in Eq. (9) expresses explicitly the dependence of the (integrated) absorption coefficient on the polarization direction of the electric field vector with respect to the oscillating dipole. It is customary to relate normal frequencies with group vibrations. Group vibrations are normal modes which encompass nuclear motions of typical nuclear configuration, like CH_3-, $-CH_2$-, keto-, carboxylic and amide groups, etc. (Bellamy, 1975).

From Eq. (9) one can conclude that infrared activity of the i-th normal vibration depends on whether at least one element of $(\delta\vec{M}/\delta q_i)_o$ is different from zero. Rigorous selection rules can be derived from symmetry considerations.

The evaluation of the molecular structure from the data of vibrational spectroscopy, e.g., from the frequencies, intensities and polarizations observed in infrared or Raman spectra, can be performed in two different but related ways. One is the rigorous analysis of the vibrational spectra of small molecules by means of normal-coordinate calculations (Herzberg, 1945; Wilson, Decius & Cross, 1955). In this treatment geometrical (conformational) parameters and parameters related to the potential energy of the molecule (force constants) are fitted to vibrational frequencies obtained from infrared or Raman spectra of a number of isotopic modifications of a given molecule. In practice, this treatment is limited by the

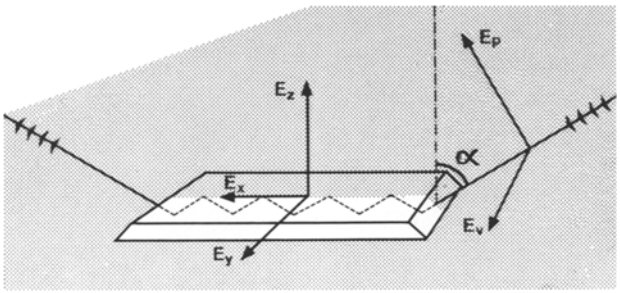

Fig. 6. ATR set-up. α: angle of incidence. E_p, E_v: parallel and perpendicular polarized components of the electric field of incident light. E_x, E_y, E_z: electric field components with respect to the coordinate system corresponding to the internal reflection plate ($E_p \rightarrow E_x$, E_z, $E_v \rightarrow E_y$)

size of the molecule: about 30 atoms are the upper limit for unsymmetrical molecules. The other way is an empirical analysis by methods of analogy, which generally is used with large molecules. However, a combination of the two methods has proved to be valuable even for structural analysis in molecules considerably larger than 30 atoms. Such a combination is reasonable because it is known from empirical analysis that some vibrational frequencies associated with a small molecule do not change significantly when this molecule becomes part of a larger one. A typical example is the quarternary ammonium group $R-\overset{+}{N}(CH_3)_3$ where a number of C-N-stretching and bending vibrations observed in the tetramethylammonium ion are found again in the hexadecyltrimethylammonium ion, in choline, acetylcholine and lecithin, respectively (Fringeli, 1977; Rihak, 1979). Therefore a normal-coordinate analysis of choline (21 atoms) was performed recently (Rihak, 1979) in order to get more detailed information on the conformation of the polar head group of lecithin (Fringeli, 1980).

Because Raman spectroscopy is less hindered by liquid water absorption than conventional infrared transmission spectroscopy, it has found a wide field of applications in biological research. This disadvantage of conventional infrared spectroscopy is largely compensated by the use of the attenuated total reflection (ATR) technique. Fig. 6 shows a schematic ATR set-up for multiple internal reflections. The sample (model membrane) is brought into close contact with the reflection plate which must be of a higher refractive index. Working above the critical angle the infrared beam is totally reflected along the plate (25–100 internal reflections are typical). From Fresnel's equations it follows that an electromagnetic field exists in the rarer medium beyond the reflecting interface, even under conditions of total reflection. This field exhibits the frequency of the incoming light, but the amplitude decreases exponentially with distance z from the surface according to $E(z) = E(0)\exp(-z/d_p)$. The penetration depth d_p is in the order of the infrared wavelength in the reflection element. The use of polarized incident light is of considerable help for the study of oriented membrane systems. As shown by Fig. 6 parallel polarized incident light (E_p) is composed of the E_x and E_z components with respect to the plate-fixed coordinate system, whereas perpendicular polarized incident light (E_v) corresponds to the $E_y$component. Molecular orientation is determined via the measurement of the dichroic ratio R which is defined as the ratio of the integrated absorption coefficients A_p and A_v with respect to parallel (p) and perpendicular (v) polarized incident light. Assuming the lipid bilayer to have liquid crystalline ultrastructure with cylindrical symmetry around the z-axis (Fig. 6), the distribution of the molecular axis with respect to the latter can be described by means of the order parameter S($S=0$ for isotropic arrangement, and $S=1$ for perfect orientation of molecular axis). The ATR dichroic ratio is given then by

$$R_z^{ATR} = \frac{A_p}{A_v} = \frac{E_x^2}{E_y^2} + \frac{E_z^2}{E_y^2}\,\frac{1+(3\cos^2\theta - 1)S}{1+(\frac{3}{2}\sin^2\theta - 1)S} \tag{10}$$

where θ denotes the angle between the transition dipole moment $\delta\bar{M}/\delta q$ and the molecular axis of the molecule. E_x, E_y and E_z are the components of the ATR field. The reader is referred to Harrick (1967) and Fringeli (1977) for more detailed information on ATR technique.

D. Neutron Diffraction

Since natural membranes are complex assemblies of different molecular species, it can be expected that a structural high resolution picture is difficult to obtain. Even in the less complex case of model membrane systems consisting of only one kind of lipid, it was not possible for a long time to look for details on the segmental level for those thermodynamic phases which are of biological interest (i.e. the gel phase and the liquid crystalline phase).

As far as diffraction methods are concerned higher resolution is only achieved when periodic arrays of elementary subunits (a lattice) exists. This is necessary since the molecular information of the elementary cell, transported by the scattered waves, is enormously amplified by the coherent scattering of the lattice. The observed intensity for a lattice is proportional to N^2, the square of the number of the cells. If the lattice is destroyed the intensity is only proportional to N. For pure lipid bilayers only the one-

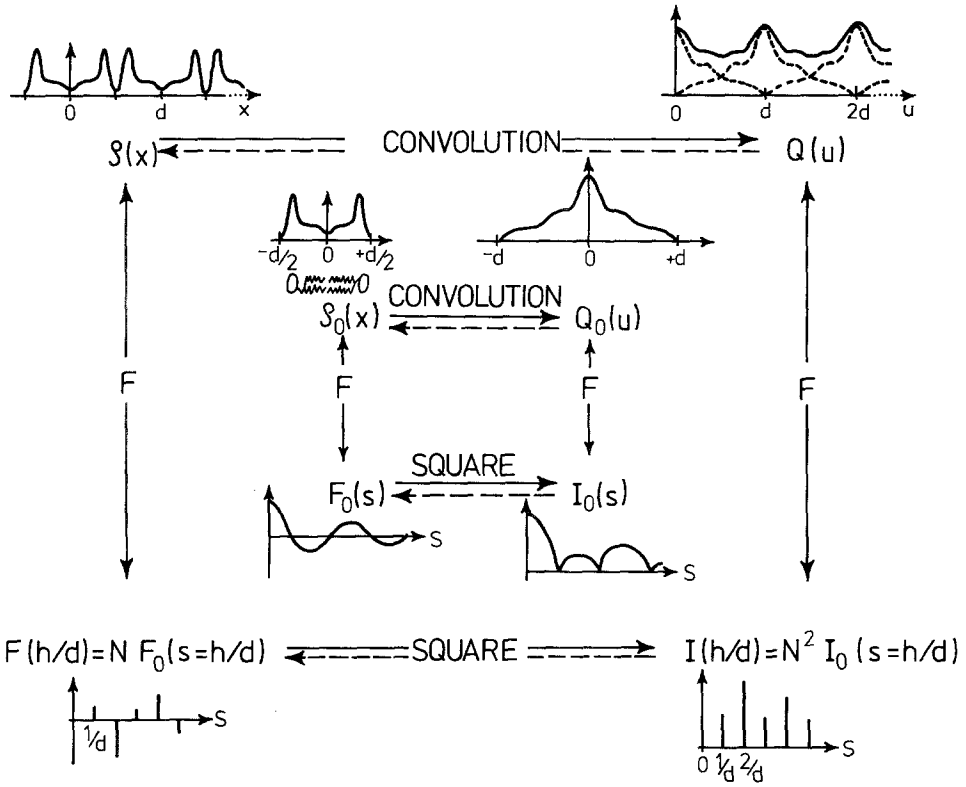

Fig. 7. The flow diagram for the profile information of a centro-symmetric planar bilayer in a diffraction experiment. The Figure consists of an inner square which illustrates the theoretical diffraction experiment on one bilayer only (which is hardly possible in reality because of intensity problems) and an outer square which shows the diffraction from a lattice of many bilayers. The one-dimensional functions $\rho_o(x)$ and $\rho(x)$ describe the profile of one bilayer and of a stack of bilayers, respectively. Diffraction on $\rho_o(x)$ and $\rho(x)$ leads to a continuous scattering amplitude $F_o(s)$ and a discontinuous amplitude $F(s=h/d)$. This is mathematically described by Fourier transforms (F). $s=2 \sin \theta/\lambda$ is the scattering parameter, where θ is the Bragg angle and λ the wavelength used; d, the lattice constant is the spacing between the bilayers and h an integer number that counts the orders. The scattering amplitude of the lattice $\rho(x)$ is determined by two factors. One is the lattice factor $G(s=h/d)$ which consists of equidistant peaks having a height proportional to N the number of elementary cells. The other factor $F_o(s)$ results from the scattering of the elementary cell (one bilayer) which modulates $G(h/d)$. Neither $F_o(s)$ nor $F(s=h/d)$ can be directly measured by a detector but only their squared values $I_o(s)$ and $I(s=h/d)$. These intensities are connected by Fourier transforms to the autocorrelation functions $Q_o(u)$ and $Q(u)$ of $\rho_o(x)$ and $\rho(x)$, respectively. $Q(u)$ is normally called the Patterson function. The broken line arrows in the Figure indicate that this operation is not a simple mathematical procedure like a Fourier transformation, but needs some additional physical information. In the diffraction experiment, $I(h/d)$ is measured and the problem is how to obtain the profile $\rho_o(x)$. This is in this simple case equivalent to the task of coming from the outer square in the diagram to a function on the inner square. For example, in swelling experiments (Franks & Lieb, 1979), the continuous intensity $I_o(s)$ is determined; in the so-called 'direct structure determination methods' (Lesslauer & Blasie, 1972; Worthington, King & McIntosh, 1973; Pape, 1974) the analysis goes via $Q(u)$ to $Q_o(u)$ which is then deconvoluted. In the neutron diffraction experiments described here $F(s=h/d)$ is determined as the square root of $I(h/d)$ and its sign obtained from an isomorphous replacement procedure (i.e., solution of the phase problem). The isomorphous sample is not produced by introducing heavy atoms into the structure but simply by changing the water between the layers from H_2O to D_2O, a process which can be controlled by the water mixture in the air (Zaccai, Blasie & Schoenborn, 1975)

dimensional lattice in the direction of the bilayer normal, which exists in multibilayer stacks, is considered. Diffraction from such a system gives information about the projection of the structure on this line (profile information). The information flow diagram for diffraction on bilayers with a center of symmetry is explained in Fig. 7. To obtain a high resolution profile, the coherently scattering multibilayer lattice should be as large as possible. The crystallographic resolution considered here is simply proportional to the number of lamellar reflections or equal to d/h_{max} (d is the interbilayer spacing and h_{max} the highest observable diffraction order). In the most favorable cases the resolution obtained from bilayers in the gel or the liquid crystalline phase was not better than 5 Å.

To understand this limitation it is useful to consider the various types of disorder which occur in these systems and cause the breakdown in the intensity at the higher reflection orders:

1. In the case of neutron diffraction, because of the large cross-sectional area of the beam, the multibilayer sample is prepared on a fairly large planar surface (e.g. a microscope slide of 2.5×6 cm). One

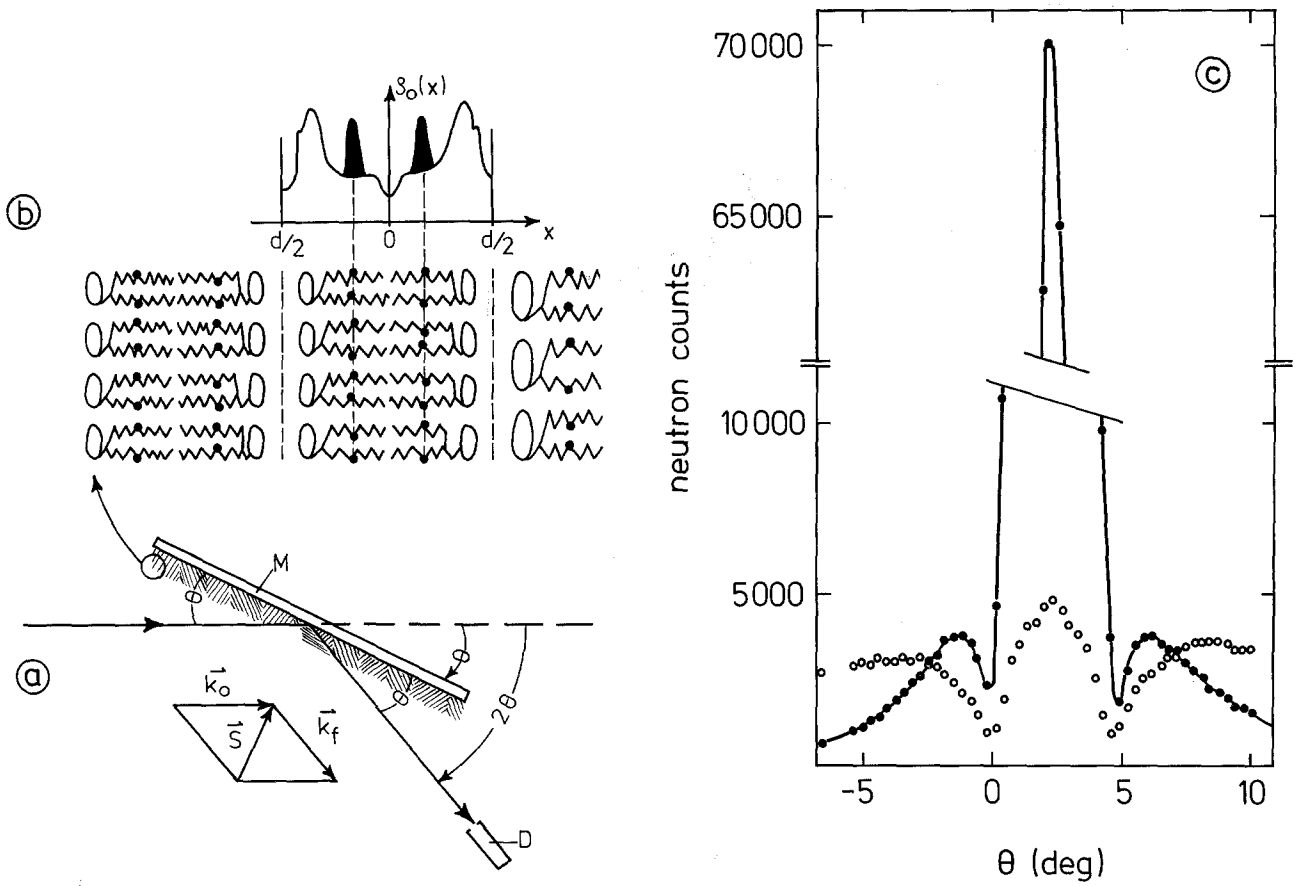

Fig. 8. Schematic presentation of a typical neutron diffraction experiment. *a*) On the slide *M* the lipid preparation is shown consisting of individual multibilayer stacks which have a certain distribution of angles with respect to the slide (mosaic spread). This distribution normally has its maximum value for multilayers parallel to the glass. Therefore, a maximum number of stacks are reflecting the neutrons in the direction of the detector *D*, when the slide is aligned in such a way that the incident beam orientation (described by the wavevector $\vec{k}_o$) has the same angle θ with the glass as the scattered beam (with direction denoted by $\vec{k}_f$). The slide is then rotated with half the angular velocity of the detector around an axis perpendicular to the $\vec{k}_o$, $\vec{k}_f$ plane at the middle of the sample ($\theta-2\theta$ scan). Thus, one after the other of the lamellar orders are recorded by the detector when Braggs's reflection condition $h/d=2\sin\theta/\lambda$ is fulfilled (Zaccai et al., 1975). *b*) Enlargement of part of a multibilayer stack. The deuterated segments are indicated by black dots. The result of the diffraction experiment and of the data reduction is an intense peak in the profile $\rho_o(x)$. *c*) Mosaic spreads of a DPPC sample with 6% (w/w) water content at 20 °C (Büldt et al., 1979). The detector was maintained at a fixed angle of 2 $\theta=4.59°$, the position of the first order ($d=57.4$ Å, $\lambda=4.6$ Å). Neutron counts are measured for different angles θ of the slide with respect to the primary beam (ω-scan). The curves are not corrected, so the dip at $\theta=0°$ is produced by absorption of the slide in the primary beam and the dip at $\theta=4.59°$ by the absorption of the slide in the secondary beam. Thus, the neutron counts qualitatively show the distribution of the multilayer stacks which have various angles with respect to the quartz slide. The distribution has its maximum at $\theta=2.30°$ for multilayer stacks parallel to the slide. Open circles show the experiments when the slide was not annealed (broad mosaic spread), and filled circles were measured with the same sample after the annealing procedure (narrow mosaic spread of $\eta\sim 3°$ full width at half-height). In this case an enhancement in intensity by a factor of 15 was obtained

method of sample preparation consists of spreading a lipid dispersion on a slide and orienting the bilayer by drying (Levine & Wilkins, 1971). The water content can be controlled by the relative humidity in the sample chamber. The whole sample does not consist of a single lattice, but is split up into many sublattices having different orientations with respect to the slide. This type of disorder can be described by the angular distribution of these individual multibilayer stacks. The full width at half-height is called the mosaic spread. If the mosaic spread is large, only a very small fraction of the sample contributes to the scattered intensity (Fig. 8*a*). When cholesterol is introduced into the membranes the mosaic spread is considerably reduced (Worcester & Franks, 1976). In some other cases a method described by Powers and Persham (1977) can be used. The sample is heated up to a high temperature and then slowly cooled (annealing procedure). In this way a very small mosaic spread can be obtained (Fig. 8*c*).

2. Another type of disorder is called lattice disorder (Schwartz, Cain, Dratz & Blasie, 1975), which occurs when there is a lack of long-range order in the lattice spacings produced by a variation in the nea-

rest neighbor distances between the bilayer; e.g., variations in the thickness of the water layer would produce this kind of perturbation. As can be expected, it is hardly possible to exclude these defects in the lattice.

3. A third type of disorder results from the thermal motions of the individual segments of the lipid molecules in the bilayer and can be approximately described by the Debye-Waller factor (Kittel, 1971). This type of disorder influences the structure factor $F_o(h)$ itself. If the mean-square displacement of a certain segment is μ^2, the structure factor of the reflection h for this segment can be written as

$$F_o(h) = 2b \exp(-2\mu^2 \pi^2 h^2/d^2) \cos(2\pi x_o h/d) \qquad (11)$$

where x_o is the mean position and b the scattering power of the segment. As is seen in Eq. (11) a large μ^2 considerably damps the scattering at higher orders via the exponential term and therefore really limits the resolution. On the other hand, for these thermodynamic phases this type of disorder is a characteristic feature of the lipid structure in the bilayer and the low resolution obtained reflects these conditions.

Unfortunately, however, X-ray profiles only show the superpositition of the broad positional distributions of the individual segements and it is not possible to localize the mean position of a certain segment or its distribution in the profile. To resolve these features, neutrons have a great advantage compared to X-rays. Using the fact that the scattering power or the coherent scattering length of deuterium ($6.67 \cdot 10^{-13}$ cm) is very different from that of hydrogen ($-3.74 \cdot 10^{-13}$ cm), a certain segment of each lipid in the bilayer is deuterated and therefore enhanced in its scattering properties without disturbing the structure. The distribution of this segment in the neutron diffraction profile can now be seen as an intense peak (Fig. 8*b*). In order to clearly resolve a deuterated segment free from overlapping effects with other groups, the difference between the profiles for a deuterated and an undeuterated specimen is taken. For many deuterated segments in the lipid molecule, it is possible to assume an *a priori* shape for the distribution in the profile. A Gaussian function was chosen for this distribution (Büldt, Gally, Seelig, Seelig & Zaccai, 1978). The choice is theoretically based on the same assumptions used for the derivation of the Debye-Waller factor (Kittel, 1971). x_o, the mean position and μ, the square root of the mean-square displacement of the label [Eq. (11)], are the two parameters of this model. The scattering amplitude can be calculated and directly fitted to the experimentally obtained difference between the structure factors for the deuterated and the undeuterated specimen. The advantage of this procedure is that the precision of the determined parameters x_o and μ is not affected by Fourier truncation errors or the influence of less precisely measured reflections which can be appropriately weighted in the fit according to their accuracy. Thus the mean position of many segments has been determined with a precision of about ± 1 Å.

III. The Glycerol Backbone as an Anchor Point for the Head Group

As seen from Fig. 2, it might be expected that the conformation of the glycerol backbone would strongly influence the structure and mobility of the head group and that this moiety may serve as an anchor point for both the fatty acyl chains and the head group. A detailed analysis of this region is therefore necessary for a proper description of the other parts of the molecule. From many observations of phospholipid molecules in the gel or liquid crystalline phase, a membrane picture has been deduced showing various types of anisotropic internal and overall motions leading to a certain degree of flexibility within the lipids and a considerable degree of disorder in the bilayer. It is clear from this description that the structure of a relatively rigid lipid molecule in a single crystal may only be used as a guide-line for the interpretation of spectroscopic and low-resolution structural data, which normally yield limited information. Let us therefore first consider the available crystal structures of *rac*-DLPE and DMPC (Hitchcock et al., 1974; Pearson & Pascher, 1979).

In both structures the glycerol backbone is oriented almost perpendicular to the layer surface, with the *sn*-1 chain (Figs. 1 and 2) continuing in this direction forming an antiplanar zigzag chain together with the glycerol moiety. The *sn*-2 chain starts first in a direction parallel to the layer and bends sharply at the second carbon atom. The torsion angles θ_1 around the C3–C2 bond in the glycerol moiety are $+58°$ (+gauche) and $+169°$ (trans) for the two DMPC conformations and $-52°$ (-gauche) in DLPE. Infrared ATR studies of dry oriented layers of DPPE and DPPC (Fringeli, 1977, 1980) confirm that the glycerol conformation is uniform in DPPE and non-uniform in DPPC. However, a new crystalline phase of DPPC monohydrate is reported, exhibiting a uniform conformation of the glycero-phosphocholine moiety (Fringeli, 1980). This suggests that no common static conformation exists with respect to this bond in the various types of phospholipid.

Are these features for the glycerol backbone of phospholipids preserved in membranes? Here the significant results are obtained from ^{2}H NMR experiments in the liquid crystalline phase. A character-

istic pattern for the quadrupole splittings of the first methylene segments in both chains of DPPC has been found (Seelig & Seelig, 1975; Haberkorn, Griffin, Meadows & Oldfield, 1977). This could be successfully interpreted as a consequence of the different conformations at the beginning of the fatty acyl chains, as seen in the crystals. The same ^2H NMR pattern was later observed in model membrane systems of DPPE, DPPG, POPC and DPPS (Seelig & Browning, 1978) and in more natural membrane systems like the elaidate-enriched membranes of *E. coli* (Gally, Pluschke, Overath & Seelig, 1979). Thus, the widespread occurrence of this pattern is a strong indication that in all these systems the glycerol backbone conformation is very similar to that found in the crystal. Neutron diffraction data have confirmed this result also for the gel state of PC (Büldt, Gally, Seelig & Zaccai, 1979) and of PE (Büldt & Seelig, 1980) by determining a positional displacement along the bilayer normal between corresponding segments in the two fatty acyl chains.

Additionally, a series of ^2H NMR data on the deuterated C3 methylene segment of the glycerol moiety gives interesting insights into the conformational and motional possibilities which exist in this region. In a first experiment on this segment in DPPC bilayers, Gally, Niederberger and Seelig (1975) obtained two quadrupole splittings with separations of 26 and 28 kHz at 45 °C. A very similar pattern for this segment was also observed in DPPS, DOPS and DPPA in the liquid crystalline state (Browning & Seelig, *unpublished results*). The synthesis of the stereospecifically deuterated C3-glycerol segment (Waespe & Seelig, *unpublished results*) allowed the conclusive assignment of the two signals of the C3-CD_2 labeled DPPC to two nonequivalent deuterons and thus rules out the possibility that the splittings were due to two long-lived conformations. Now two possibilities can be seen to interpret these patterns (Wohlgemuth, *unpublished results*). Firstly, these splittings can be easily approached using the rigid crystallographic conformation together with the rotator motion of the lipid. Secondly, this model can be extended in the following way. The nonequivalence of the two deuterons excludes the possibility of rapid rotation around the C3-C2 axis covering the whole angular range, because such a motion would lead to the same average EFG tensor for both deuterons. A slow rotation (compared to the ^2H NMR time scale) in the whole angular range would also not explain the observed quadrupole splittings, since the same superposition for the different C-D orientations, occurring during the slow rotation, would be obtained for both deuterons. However, a rapid or slow oscillatory motion with restricted angular amplitude would still be possible. Thus, the correlation time of 2.1×10^{-10} sec for this segment of DPPC in the fluid state at 51 °C, derived from T_1 relaxation time measurements using the isotropic approximation (Brown & Seelig, 1978), can originate from different types of motions, namely rotator and small wobbling motions of the whole molecule as well as the above-mentioned rapid oscillatory motion. In any case the mobility of this segment is reduced by a factor of three compared to the adjacent fatty acyl chain segments, even though the ordering (as measured by the quadruple splitting) is practically identical.

In conclusion, the ^2H NMR patterns of the first methylene segments in the fatty acyl chains and the C3-glycerol splittings together with the relatively long correlation time for this segment, justify the picture of the glycerol moiety as the most rigid part of the various phospholipids investigated.

IV. A Static and Dynamic Picture of the Head Group

A. Single crystals

As in the last section, a discussion of the results of the single-crystal structures will be given first. The unit cell of DMPC contains two molecules of conformation A and two of B, which differ mainly with respect to the torsion angles of their polar head groups (Table 1). These are approximately mirror images of each other. In the case of the *rac*-DLPE crystal structure, the unit cell contains mirror images of the whole phospholipid molecule, which is possible because *rac*-DLPE is a mixture of lipids differing in the configuration of the C2-glycerol segment. Therefore, only one set of torsion angles has been given

Table 1. Torsion angles of crystallographically determined phospholid headgroup structures

Phospholipid		θ_1	α_1	α_2	α_3	α_4	α_5
rac-1,2-dilauroyl-glycero-3-phosphoethanolamine · CH_3COOH (Elder et al., 1977)		−52	−154	58	66	106	67
1,2-dimyristoyl-*sn*-glycero-3-phosphocholine · $2H_2O$ (Pearson & Pascher, 1979)	A	58	162	68	63	139	−51
	B	169	170	−76	−46	−161	64

(Table 1). The internal structure of the DLPE and DMPC head groups are quite different according to the torsion angles in Table 1. Both molecules of DMPC show the tendency of the nitrogen to fold back towards the phosphate group, so as to minimize the distance between the groups of opposite charge. On the other hand, the DLPE head group has a more extended conformation.

The intermolecular connections due to hydrogen bonds are different in the two structures. In the DLPE crystals, which contained no water, hydrogen bonds (2.8 Å long) are formed between the nitrogen and the nonesterified phosphate oxygen atoms of adjacent molecules. In DMPC the nitrogen atom comes no closer to the phosphate oxygens than 4.5 Å because of the bulky choline group. These DMPC crystals include two water molecules per lipid, which are used to form the intermolecular connections by hydrogen bonds. For instance, the phosphate groups of molecules A and B in the asymmetric part of the unit cell are linked by the following hydrogen bond pattern: phosphate (A)-water-phosphate (B)-water. It has often been suggested that differences in the water structure may cause changes in the headgroup conformation. Therefore, the DMPC crystal data provide an illustrative example of how the water structure is used to link neighboring lipids in the interfacial region. Unfortunately, as the DLPE crystal contained no water, the interesting comparison of possible different water structures cannot be made. The fact that DLPE forms hydrogen bonds without the use of water is in agreement with the observation that PE-bilayers take up very little water from air humidity, contrary to the behavior of PC.

A *common feature* of the head groups of both crystal structures is the overall orientation and length of the P-N distance vector, which is inclined to the bilayer plane at small angles [17°; 4.3 Å and 27°; 4.5 Å for DMPC (Pearson & Pascher, 1979) and 15°; 4.4 Å for DLPE (Elder et al., 1977)].

B. Membranes

Having analyzed the glycerol group and the crystallographic data, the conformational picture of the various polar head groups will now be discussed. The phosphate group is not only the connecting link between the head group and the glycerol part, but it may also play a role in stabilizing the membrane by its ability to initiate via water molecules a hydrogen bond network to neighboring lipid molecules, as was seen in the DMPC crystals. The main experimental tool for these studies is ^{31}P NMR using the phosphorus atom itself as a natural label.

1. The Phosphodiester Part

Let us first consider phospholipid phases which exhibit almost no rotator and internal motions. Griffin, Powers and Pershan (1978) have investigated oriented DPPC monohydrate specimens using ^{31}P NMR where the lipid was in the crystalline phase at room temperature. From the orientation of the σ_{11} component of the shift tensor, an angle of $50° \pm 5°$ of the O-P-O plane (where the O's are the nonesterified oxygens of the phosphodiester part) with respect to the bilayer normal was determined. In addition, the mean orientation of the σ_{33} component indicated that the line between the nonesterified oxygens is approximately oriented parallel to the bilayer plane. This agrees with the structure in the DLPE single crystal. Attenuated total reflection infrared spectroscopy (ATR) by Fringeli (1977) for DPPC and DPPE and infrared transmission studies on DPPE by Akutsu, Kyogoku, Nakahara and Fukuda (1975) have confirmed these results. More recently, Fringeli (1980) has shown that a uniform conformation of the phosphodiester part of DPPC exists in the crystalline monohydrate. This phase becomes unstable as soon as the water content of the layer is enhanced. Therefore, one has to assume at least two different conformations for the phosphate moiety of DPPC under biologically relevant conditions.

The conformation of the phosphodiester part is now examined in phases where different kinds of motions occur. Recent ^{2}H NMR measurements on DPPC bilayers (Davis, 1979) have shown that rotator motions of the whole molecule around its long axis disappear on the ^{2}H NMR time scale at temperatures below -7 °C. From ^{31}P NMR investigations on fully hydrated DPPC bilayers at -10 °C (Herzfeld et al., 1978), a chemical shift anisotropy $\Delta\sigma = -69$ ppm was observed, which can be explained by the same conformation of the phosphate group as in the immobilized state, together with a rapid motion of this group around the director axis. Since in this case the ^{31}P NMR and ^{2}H NMR time scales are comparable, the above-mentioned experiments suggest that under these conditions the value of the chemical shift anisotropy reflects the rotator motion.

At higher temperatures other types of motions come into play. Thus, the order of the phosphate group, as studied by ^{31}P NMR, traces phase transitions, as seen in Fig. 6, where the temperature dependence of $\Delta\sigma$ is shown. In low temperature phases, where the motions are practically frozen in, identical static chemical shift tensors were observed (*compare* section II). However, Fig. 9 illustrates at higher temperatures differences in the $\Delta\sigma$ values are observed for the individual phospholipids. For instance, the

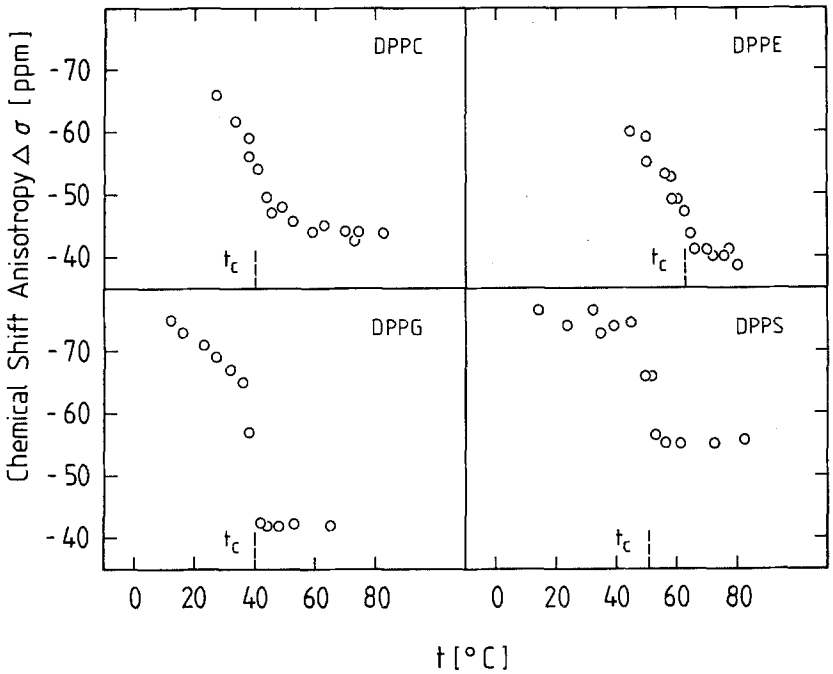

Fig. 9. Variation of ^{31}P chemical shift anisotropy (in parts per million) with temperature for unsonicated bilayers of four phospholipids differing in their head groups. DPPC and DPPE were measured at a lipid:buffer ratio of 50:50 wt%. The buffer consisted of 0.2 M sodium acetate/acetic acid (pH 5.7) and 10^{-4} M EDTA (Brown & Seelig, 1978). DPPG in the naturally occurring 3,1'-configuration was dispersed as the sodium salt in 0.1 M NaCl to form a dispersion with 50 wt% lipid at pH 7 (Wohlgemuth et al., 1980). DPPS (in the naturally occurring L-L-configuration) was also dispersed as the sodium salt in 0.1 M NaCl, but with excess buffer consiting of 0.05 M N-2-hydroxyethylpiperazine-N'-2-ethanesulfonic acid, sodium salt-Tris at pH 7 and 10^{-3} M EDTA (Browning & Seelig, 1980)

measured chemical shift anisotropies in the fluid phase can be arranged in the following order: −40 ppm for DPPE (Seelig & Gally, 1967), −41 ppm for DPPG (Wohlgemuth, Waespe-Šarčevic & Seelig, 1980), −45 ppm for DPPC (Gally et al., 1975) and −55 ppm for DPPS (Browning & Seelig, 1980). These variations of the $\Delta\sigma$ values can reflect conformational and/or motional differences for these lipid species with respect to the phosphate group. According to Eq. (8), $\Delta\sigma$ can be used to determine a mean orientation of the phosphodiester part, if one of the two order parameters is known from other methods. For instance, infrared dichroism of the O3−P−O4 antisymmetric stretching vibration could in principle determine S_{33} (Akutsu et al., 1975). Unfortunately, such data are not available in the fluid phase, so that a quantitative description is not as yet possible. However, a correlation of the $^{31}P-T_1$ relaxation times with the $\Delta\sigma$ values allows a qualitative estimation of differences in the motional contributions to the $\Delta\sigma$ values of these phospholipid species. Thus, by a comparison of $^{31}P-T_1$ relaxation times of phosphatidylserine with the other lipids, Browning and Seelig (1980) have suggested that the PS head group is more rigid than the other head groups which would be in agreement with the observed larger chemical shift anisotropy of PS.

So far different head groups of phospholipids having the same fatty acyl chains have been considered. However, studies of phospholipids carrying the same head group have shown that variations in the fatty acyl chainlengths or in the degree of unsaturation do not influence the ^{31}P NMR results appreciably (Seelig, 1978; Browning & Seelig, 1980).

2. Individual and Common Features of Various Head Groups

The Overall Orientation of the Phosphocholine Group. First the work will be reviewed which has determined the *overall orientation* of the polar head group.

Extensive neutron diffraction studies in the gel and liquid crystalline phase on bilayers with different degrees of hydration were performed on selectively deuterated DPPC systems. (Büldt et al., 1978, 1979; Zaccai, Büldt, Seelig & Seelig, 1979). These investigations give a time-averaged picture of the mean conformation and of the disorder along the bilayer normal. As an example of these studies Fig. 10 shows scattering profiles of the β-CD_2 deuterated DPPC in comparison with undeuterated DPPC for the gel and the fluid phase. In Table 2 the obtained parameters describing the distribution of the deuterated headgroup segments along the bilayer normal are summarized in the case of DPPC. The general result, seen in Table 2, is that under all conditions investigated the headgroup positions Cα, Cβ and Cγ are very close together, which proves that the phosphocholine

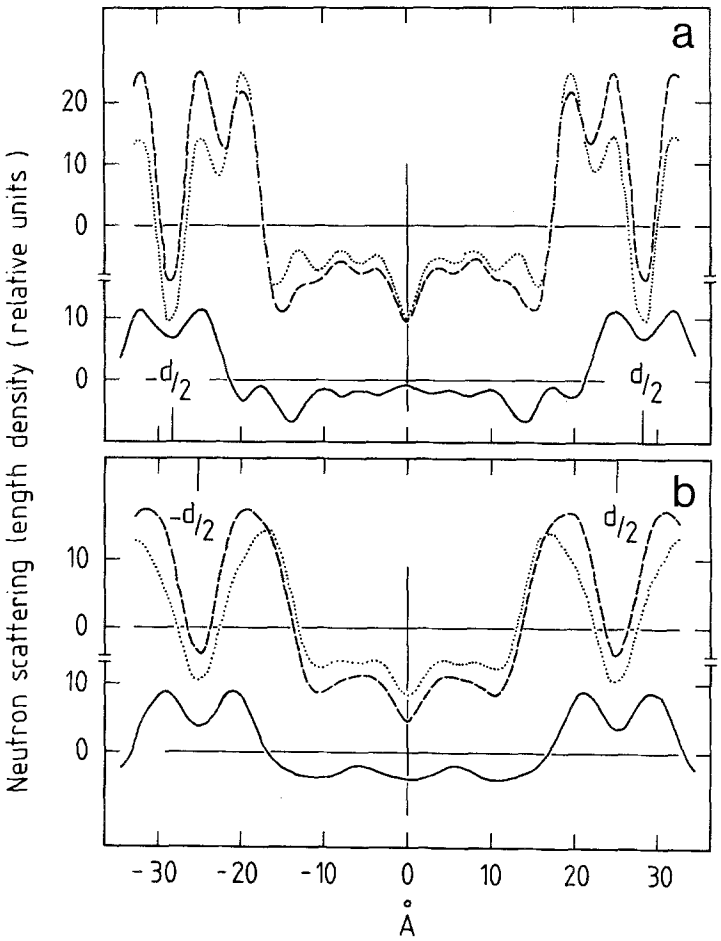

Fig. 10. Neutron scattering length density profiles for oriented multilamellar samples of β-CD_2 deuterated DPPC (---) and undeuterated DPPC (.....). The difference between these profiles (———) shows the mean position and distribution of the β-CD_2 segment along the bilayer normal. (*a*) Profiles of DPPC bilayers in the gel phase with 6 wt% H_2O at 20 °C, having a lamellar spacing of 57.4 Å. (*b*) Profiles of DPPC bilayers in the liquid crystalline phase with 10 wt% H_2O at 70 °C, having a lamellar spacing of 50.8 Å

groups are oriented almost parallel to the bilayer surface. This is further substantiated by comparing the experimental results with the corresponding distances measured form a space-filling molecular model (column 3, Table 2a). The phosphocholine head groups were either aligned parallel or extended perpendicular to the bilayer surface. The difference in the positions of the Cγ segments for the two orientations in the model is 5.2 Å, where the Cγ position measured is the center of mass of the nine deuterons in the three methyl groups. The Cγ segment represents the strongest label in the molecule, therefore its mean position has been determined with high accuracy to be $x_0 = (25.1 \pm 0.6)$ Å (first column Table 2*a*). This value alone is a strong argument for the P-N vector to be aligned almost parallel to the bilayer plane. The width μ of the label distribution, which is a measure of the positional fluctuations along the bilayer normal, has been obtained from some diffraction patterns of higher resolution. At first glance, considering the Cβ segment, the values of $\mu = 2.1$ Å for the gel phase and of $\mu = 2.6$ Å for the fluid phase suggest a high degree of fluctuation in the orientation of the P-N vector. But if the connecting vector of the two deuterons of this segment is oriented perpendicular to the bilayer surface with a length of 2.2 Å, this would give a value of 2.0 Å, taking into account the mean fluctuation 0.9 Å of the whole molecule along the bilayer normal as seen from the C2(1) segment. Thus, without assuming much variation in the angle between the P-N vector and the plane of the bilayer, a width of 2.1 or 2.6 Å can be explained.

The overlap in the profiles of the Cβ segments in Fig. 7 reminds us of the fact that interactions between the head groups of neighboring layers occur. Therefore, it is important to investigate the question whether this orientation of the P-N vector is mainly caused by interactions between head groups in the same layer or by interactions with head groups in the adjacent layer. Increasing the hydration of the DPPC membrane from 6 or 10 to 25 wt%, as shown in Table 2, did not alter the orientation of the dipole within the accuracy of the measurements. However, a clear answer to this question has been found from experiments on single shell vesicles studying the $^{31}P\{^1H\}$ nuclear Overhauser effects (NOE). (Yeagle, Hutton, Huang & Martin, 1976; Yeagle, 1978). In these experiments dipole-dipole relaxation between the phosphate and the choline methyl groups of different lipid molecules was investigated, which led to the result that both groups are on average very

Table 2. Summary of the results in the headgroup region of DPPC

(*a*) The gel phase

	6 wt% H_2O, 20 °C, d = 57.4 Å					25 wt%, 28 °C, d = 62.5 Å
	oriented (mosaic spread ~ 20°)	highly oriented (mosaic spread ~ 1°)		x_0 values determined from a space-filling model		powder
	x_0 (Å)	x_0 (Å)	μ (Å)	head ∥ surface	head ⊥ surface	x_0 (Å)
Cγ	25.1 ± 0.6			24.4	29.6	24.4 ± 0.6
Cβ	24.8 ± 0.7	25.3 ± 0.6	2.1 ± 0.5	25.3	28.0	24.1 ± 1.0
Cα	24.5 ± 0.7			24.0	27.2	23.6 ± 1.0
C3	23.1 ± 1.0			23.5		21.6 ± 1.5
C2(1)		18.4 ± 0.6	0.9 ± 0.4			

(*b*) The liquid crystalline phase

	10 wt% H_2O, 70 °C, d = 50.8 Å highly oriented (mosaic spread ~ 1°)		25 wt% H_2O, 50 °C, d = 54.1 Å powder
	x_0 (Å)	μ (Å)	x_0 (Å)
Cγ			21.8 ± 0.6
Cβ	21.3 ± 0.6	2.6 ± 0.6	21.2 ± 1.0
Cα			21.0 ± 1.0
C3			17.4 ± 1.5

C2(1) is the second carbon atom in the *sn*-1 chain.
x_0 is the mean position of the deuterated segment, as measured from the hydrocarbon center of the bilayer.
μ is the square root of the mean-square displacement of the segment along the bilayer normal or $\sqrt{2} \cdot \mu$ is the half-width at 1/*e* height of the distribution of the deuterated segment along the bilayer normal.

close together. This effect is a proof for the orientation of the P-N vector parallel to the bilayer plane and was found for the phosphocholine dipoles in vesicles of egg-yolk lecithin (egg PC). In vesicles containing mixtures of egg PC with cardiolipin and of egg PC with PE, the ^{31}P NOE was obtained as for pure egg PC and therefore these studies demonstrate that the methyl protons of the choline group interact closely with the phosphate of the other lipids in the mixtures as well as with those of PC. These findings were further substantiated by the observations that increasing amounts of cholesterol cause a weakening of the intermolecular headgroup interactions, which is explained by the spacing effect of cholesterol (Yeagle, Hutton, Huang & Martin, 1975). In conclusion, these experiments on single shell vesicles give convincing evidence that interaction forces in the interfacial region of one bilayer alone result in an orientation of the zwitterionic headgroups parallel to the membrane surface.

The Overall Motion of the Phosphocholine Group. Having discussed studies on the mean orientation of the phosphocholine P-N vector, a method will now be presented suitable for observing the mobility of this vector. Many phospholipids carry a zwitterionic headgroup, which results in a fairly large permanent dipole moment (about 18 Debye in the case of PC). For these lipids the dipole is a very useful natural probe for dielectric relaxation investigations to study the motion of this group and to trace the influence of phase transitions or overall changes of the membrane in the polar region. Thus, using the headgroup dipole of DPPC, the effect of the pre- and main transition on the motion of the dipole was clearly resolved (Shepherd & Büldt, 1978). The relaxation frequency in the case of DPPC increases from 10 MHz to 80 MHz during the change from the gel to the liquid crystalline phase, reflecting the decrease in the intermolecular interactions due to the increased distances between neighboring head groups. A considerable restriction in movement still exists at temperatures higher than the main phase transition temperature, because the relaxation frequency is still increasing with temperature. If cholesterol is introduced into the bilayer, neighboring head groups should be more separated due to the spacing effect of the cholesterol molecules. Neutron diffraction studies (Worcester & Franks, 1976) suggest that cholesterol does not *directly* interact with the headgroups of egg lecithin because the oxygen in the cholesterol head group is positioned near to the glycerol-fatty acid ester bonds of the phospholipid. Dielectric investigations on DPPC multilayers containing increasing amounts of

cholesterol showed that the rate of the phosphocholine dipole motion increases in the gel phase. In the fluid phase the relaxation frequency first decreases at low cholesterol content, then after reaching a minimum value between 20 and 30 mol% increases by addition of more cholesterol (Shepherd & Büldt, 1979). This behavior can be partly accounted for by the increase of chain order due to cholesterol and possibly changes in the water structure may play a role. It is interesting to note that ^{2}H NMR splittings observed in systems of Cγ deuterated DPPC and cholesterol show a corresponding behavior above the phase transition (Oldfield, Meadows, Rice & Jacobs, 1978).

Extensive dielectric studies on DMPC and DPPC multilayered liposomes, which considered headgroup motion as well as water relaxation, have been reported by Kaatze, Henze and Eibl, (1979) and Kaatze, Henze and Pottel (1979). Interesting results were obtained from investigations on various DPPC analogs carrying up to 10 methylene segments in the zwitterionic headgroup between the phosphate and the nitrogen. The mobility of the dipole decreases for head groups containing up to 8 CH_2 segments and then slowly increased for head groups having more segments. A singularity exists in this behavior for head groups with 6 DH_2-groups. The mobility of this compound is the same as for naturally occurring DPPC with 2CH_2 groups. Here a special unknown conformation with increased motion is assumed. The main points which seem to contribute to the behavior of the mobility of these compounds, are (a) the increased friction due to the lengthening of the head group, which is partly compensated due to a higher internal flexibility with increasing numbers of methylene segments, and (b) changes in the geometry and interaction between the head groups.

The Conformational and Motional Details of Various Head Groups. The results mentioned above in this section concerned the overall orientation and motion of the polar head group. From infrared dichroism measurements on dry oriented multilayers of DPPE, Akutsu et al. (1975) have obtained orientational information of some segments. With respect to the head group, the Cα-N vector has been found almost parallel to the bilayer surface assuming a gauche conformation of the O-C-C-N^+ group. Based on ATR infrared spectroscopy, also on dry multilayers, Fringeli (1977) concluded that the mean deviation of the Cα–Cβ bond from the plane of the bilayer is between 0–50° for DPPE and DPPC. In the single crystal structure of DLPE this angle was determined to be 29°.

For the biologically interesting liquid crystalline phase ^{2}H NMR experiments have yielded many details of phospholipid structure and motion. Considering segmental order parameters in the chain region, a unique interpretation was possible. In this case, assuming rapid trans-gauche isomerization, the order parameters of the individual segments reflect a certain average of the amplitudes of these fluctuations and on the basis of a theoretical model can yield the most probable spectrum of chain conformations (Marčelja, 1974; Schindler & Seelig, 1975; Meraldi & Schlitter, 1980). The success in the interpretation was due to the chemical structure of chains leading to simplifying assumptions with respect to the different kinds of interaction forces. In contrast, the polar region is chemically more complex resulting in a complicated pattern of interactions. For instance, some of the phospholipids have different charges in the head group, which change the electrostatic interactions. In addition, the hydrogen bond network and the water structures for various head groups may be different. These forces act on each segment in an unknown way. Mainly because of the lack of symmetry it is difficult to predict the contributions of the motional and conformational parts of the order parameters. Therefore, it was necessary to interpret the results considering certain molecular models, which in combination with deuterium T_1 relaxation times can lead to the exclusion of some extreme cases.

Firstly, the experimental results will be summarized. Complete sets of data are available for phosphatidylcholine (Gally et al., 1975), phosphatidylethanolamine (Seelig & Gally, 1976), phosphatidylglycerol (Wohlgemuth et al., 1980) and phosphatidylserine (Browning & Seelig, 1980). The head group of phosphatidylglycerol is an illustrative example, showing the quadrupole splittings of the individual segments and simultaneously demonstrating the sensitivity of ^{2}H NMR for slightly different structures (Fig. 8). In contrast to PC and PE, the head groups of PG and PS contain a second asymmetric carbon atom at the Cβ position in addition to the C2 segment in the glycerol backbone. As an example Fig. 8(*a*) shows a ^{2}H NMR spectrum of DPPG with a perdeuterated glycerol head group containing a 1:1 mixture of two diastereomers (having the same glycerol backbone configuration). The assignment of the splittings is achieved by synthesis of selectively labeled DPPG's (Fig. 11*b* to *d*). The quadrupole splittings $\Delta\nu_Q$ decrease in the order Cα, Cβ, Cγ. The broad width of the absorption lines of the α-CD_2 group in Fig. 11*a* is explained by the superposition of the powder patterns of the two diastereomeric configurations, each of which is plotted in Fig. 11*c* and *d*. The spectrum of one of the diastereomers (Fig. 11*c*) is composed of two overlapping powder patterns with

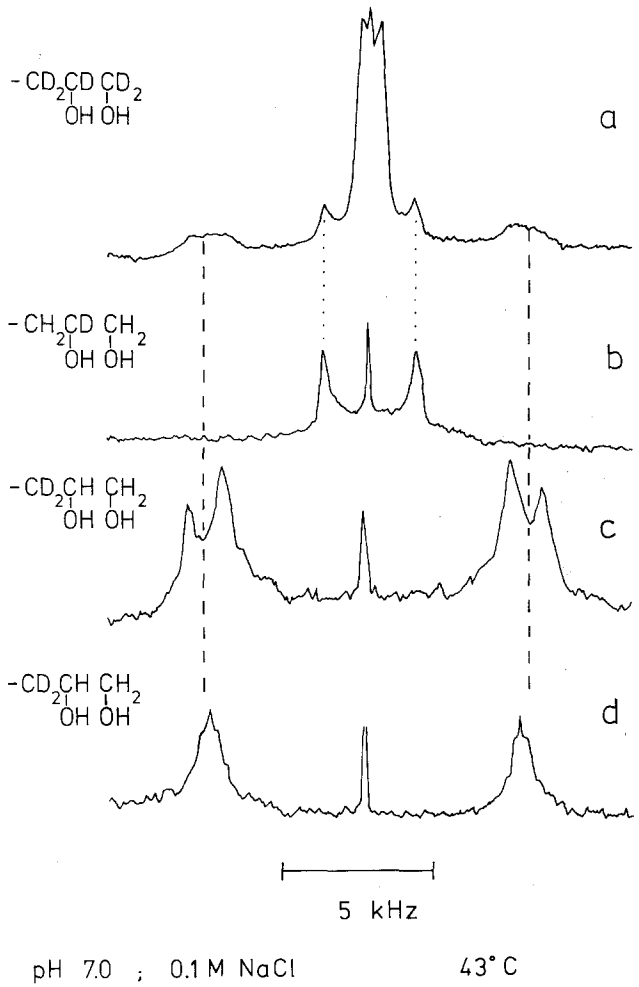

Fig. 11. Deuterium magnetic resonance spectra (61.4 MHz) of unsonicated DPPG-bilayers (15 wt% lipid) in excess PIPES-buffer (pH 7.0) and 0.1 M NaCl at 43 °C. For each sample 30 mg (dry wt) of phospholipid was used. The site(s) of deuteration in the glycerol head group are shown on the left side. (*a*) and (*b*) refer to corresponding deuterated derivatives of 1,2-dipalmitoyl-*sn*-glycero-3-phospho-*rac*'-glycerol, while the DPPG in (*c*) had the 3'-glycerol head group (also designated as D-configuration) and in (*d*) the naturally occurring 1'-glycerol configuration (L-configuration at the Cβ position)

slightly different quadrupole splittings which have been shown to arise from the two nonequivalent deuterons and not from a long-lived conformational equilibrium in the head group. However, the other diastereomer, which is the naturally occurring one, shows only one splitting. Two signals at the α-CD_2 headgroup positions are characterisitc also for the other three head groups mentioned above, although for PE and PC the splittings are close together and are difficult to resolve (Akutsu & Seelig, *unpublished data*). It is probable also in these cases that the two splittings originate from two nonequivalent deuterons. Fig. 12*a* shows a summary of $\Delta\nu_Q$ values for the α-CD_2 segment of the four different head groups. The difference in the two splittings increases from PC to PS with a particularly large difference between the two splittings in PS. This behavior could either be caused by slight conformational changes in a more rigid headgroup structure or by a decrease in the amplitude of fluctuations. As seen in Fig. 12*b* the splittings of the β-CD_2 segments are similar in the case of PC, PE and PG but the $\Delta\nu_Q$ value is greatly increased in the case of PS. Table 3 summarizes the observed quadrupole splittings of the four phospholipids at corresponding temperatures, i.e. 5 °C above the respective gel-to-liquid crystalline phase transition temperature. Included are the $\Delta\nu_Q$ values of the Cγ positions for PC and PG, which are relatively small. The two splittings observed in the Cγ position of PG have not yet been assigned.

The interpretation of the deuterium quadrupole splittings and the phosphorus chemical shift anisotropies proceeds by conceiving physically reasonable models for the headgroup structure and flexibility and by calculating the $\Delta\nu_Q$ and $\Delta\sigma$ values on the basis of these models. Two extreme cases may first be considered:

1. *Free rotation* around all bonds of the phosphocholine headgroup was discussed by Seelig, Gally and Wohlgemuth (1977) and Kohler and Klein (1977). This concept was ruled out by not fitting the observed data, as can be seen already from the low calculated chemical shift anisotropy $\Delta\sigma = -5.1$ ppm. This value was determined using the shift tensor of Kohler and Klein (1977), with the assumption that the most probable C2-C3-orientation is parallel to the bilayer normal and that there is (on the ^{31}P-NMR time scale) a rapid rotation around the C2-C3-axis. However, even when there is no rotation around the C2-C3-axis and this axis is not parallel to the bilayer normal (compare section III), the observed chemical shift anisotropies cannot be explained ($|\Delta\sigma_{Calc}| < 14$ ppm). The use of the refined orientation data obtained from the BDEP-shift tensor (Herzfeld et al., 1978) does not change the calculated $\Delta\sigma$ for this model appreciably. It is obvious that the model of free rotation is excluded for the other phospholipids as well, since the measured chemical shift anisotropies range between -40 and -80 ppm (*compare* Table 3 and Fig. 6)

2. In a *rigid molecule* analysis assuming only rotator motion it was shown (R. Wohlgemuth, *unpublished results*) that the observed $\Delta\nu_Q$ values as well as the $\Delta\sigma$ values could be fitted. The number of possible sets of torsion angles in these calculations is very different for the individual phospholipids according to the different numbers of available deuterable sites. Some of the conformations had angles similar to those observed in the single-crystal struc-

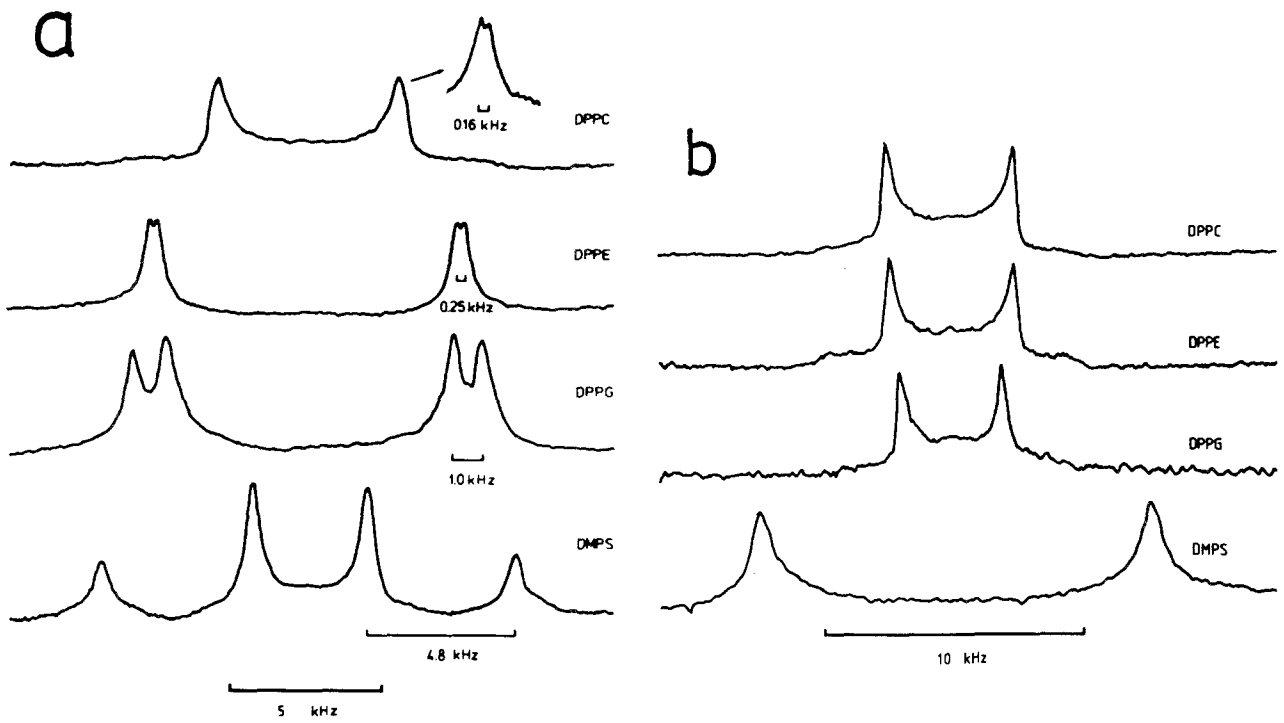

Fig. 12. Comparison of ^2H NMR spectra of DPPC, DPPE, L,L-DPPG (3,3'-DPPG in the other nomenclature) and L,L-DPPS in the liquid crystalline state, deuterated in the Cα (Fig. 12*a*) and the Cβ-position of (Fig. 12*b*) of the head group

Table 3. Comparison of the phosphorus chemical shift anisotropy $\Delta\sigma$ and the deuterium quadrupole splittings $\Delta\nu$ of naturally occurring phospholipid head groups*

Head group (compound)	T_c (°C)	$\Delta\sigma$ (ppm)	$\lvert\Delta\nu\rvert$ (kHz) α	(kHz) β	(kHz) γ	Ref.
Phosphocholine		P–O–CH_2–CH_2–$\overset{+}{N}$–$(CH_3)_3$				a, b
(DPPC)	41	−47	6.0	5.3	1.2	
Phosphoglycerol		P–O–CH_2–C(H, Δ, OH)–CH_2–OH				c
(L, D-DPPG or						
3,1'-DPPG)	41	−41.5	10.3	3.3	0.5 0.8	
Phosphoethanol-		P–O–CH_2–CH_2–$\overset{+}{N}H_3$				d, e
Amine (DPPE)	63	−41	10.3 9.8	3.7		
Phosphoserine		P–O–CH_2–C(H, Δ, COO^-)–$\overset{+}{N}H_3$				f
(L, L-DMPS)	36	−55	13.7 4.1	15.4		

* Data are compared at corresponding temperatures, i.e., 5 °C above the respective gel-to-liquid crystalline transition temperatures.

[a] Gally et al., 1975.
[b] Seelig et al., 1977.
[c] Wohlgemuth et al., 1980.
[d] Seelig and Gally, 1976.
[e] Akutsu and Seelig, *unpublished results*.
[f] Browning and Seelig, 1980.

ture of *rac*-DLPE (*see* Table 1). In PC the N-methyl-groups were allowed only to rotate around the CH_3-N axis but the $N(CH_3)_3$ group as a whole was kept fixed. The observed changes of the experimental data with temperature could be accounted for by small conformational changes. However, assuming isotropy in the rate of motions, the observed larger T_1 deuterium relaxation times for Cα and Cβ deuterons compared to those of the C3-glycerol position in PC would exclude this rigid headgroup model and suggest increasing flexibility towards the Cγ position. (Gally et al., 1975; Brown, Seelig & Häberlen, 1979; *compare also* ^{13}C T_1 results of Lee, Birdsall, Metcalfe, Warren & Roberts, 1976). A more quantitative analysis would require the determination of the spectral densities.

3. Between these extreme cases an infinitely large number of other possible models can be constructed, also fitting the available data. In crystal structures of *sn*-glycero-3-phosphocholine (Abrahamsson & Pascher, 1966) two enantiomeric conformations of the phosphocholine group were found, which has led to the idea that these conformations could also be the most probable ones in the liquid crystalline phase, additionally assuming rapid transitions between these two states. Indeed this model could explain the observed $\Delta\nu_Q$ and $\Delta\sigma$ values (Seelig et al., 1977). This concept was further confirmed by the observation of two enantiometric conformations in the crystal struc-

ture of DMPC (Pearson & Pascher, 1979). However, it should be noted that many possible enantiometric conformations exist and that the available data only exclude certain regions in the conformational space of this model (Skarjune & Oldfield, 1980). In the above calculations the C2–C3 axis of the glycerol moiety was assumed to be the axis of rotation and that its most probable alignment was parallel to the director axis. In section III it was shown that the two C3–CD_2 deuterons are not equivalent which underlines the approximate character of these assumptions.

Infrared ATR spectra of DPPC give further evidence that the phosphocholine part assumes conformations different from all-gauche$^+$ and all-gauche$^-$, respectively (Fringeli, 1977). Based on normal-coordinate analysis of choline and related compounds (Rihak, 1979) it was shown that in both, the crystalline and the liquid crystalline state of DPPC, about 10% of the O-C-C-N fragment assumes a conformation different from g^+ and g^-. These 10% might be considered as intermediates of the $g^+ \rightleftarrows g^-$ transitions which could be resolved because of the high time resolution ($\sim 10^{-13}$ sec) of vibrational spectroscopy. Infrared ATR spectroscopy reveals uniform choline headgroup conformation only for a distinct phase of DPPC monohydrate (Fringeli, 1980).

Without using models some features can be deduced by comparing the results from the four phospholipids in Fig. 11, Fig. 12 and Table 2. This will be shown for the case of PS.

(a) The difference in the quadrupole splittings observed for the two α-CD_2 deuterons is 10 kHz, whereas for the other compounds it does not exceed 2 kHz. This dramatic nonequivalence of the deuterons indicates their relatively reduced motional averaging.

(b) The quadrupole splitting of the β-CD segment is found to be 15.4 kHz for PS while the measured splittings of the others are in the range of 3–5.5 kHz.

(c) The ^{31}P and ^2H T_1-relaxation times in the PS head group are considerably shorter than in the PC and PE head group (Browning & Seelig, 1980).

Each of these three facts alone is not a significant proof for internal rigidity in the PS head group, but the coincidence of these observations suggests a relatively rigid internal headgroup structure for PS. This rigidity is probably the result of differences in the electrostatic interactions and in the hydrogen-bonding network within the phosphatidylserine polar region. Since these forces should be different for DMPS and DMPC, bilayers containing a mixture of these lipids should have an altered interaction pattern. Indeed, dilution of DMPS with neutral DMPC showed decreased quadrupole splittings for the head groups of DMPS, similar to those observed in pure PC and PE. This suggests that dilution of negatively charged DMPS with neutral DMPC reduces these interactions and allows for greater freedom of motion of the PS head group (Browning & Seelig, 1980). It is interesting to note that the two headgroup diastereomers of both PG and PS have the same quadrupole splitting for the Cβ position, but show differences for the α-CD_2-segment (e.g. Fig. 11 *c* and *d*).

In all the phospholipids mentioned above, the polar head group is attached to the C3 position of the glycerol backbone, as is the case for natural phospholipids. In 1,3-dipalmitoyl-*sn*-glycero-2-phosphocholine (2-*sn*-DPPC), which is not naturally occurring, one chain is attached to the C3 position of the glycerol backbone, the other chain remains at the C1 position, while the head group is connected to the C2 position. It was found (Seelig, Dijkman & de Haas, 1980) that this compound has similar thermodynamic properties as 1,2-dipalmitoyl-*sn*-glycero-3-phosphocholine (DPPC). (The correct abbreviation in this case would be 3-*sn*-DPPC, but to follow the nomenclature used up to now, we will continue to call this structure DPPC). The glycerol part of 2-*sn*-DPPC is chemically symmetric and it may be expected that this leads also to a corresponding symmetry in the structure. Indeed, one quadrupole splitting is observed for the first methylene segments in both chains of 2-*sn*-DPPC. The value is in agreement with the average quadrupole splitting of this segment in the *sn*-2 chain of DPPC. This strongly supports the idea that both chains in 2-*sn*-DPPC have a bent chain conformation. The larger area per molecule of 2-*sn*-DPPC compared to DPPC, as determined in monolayer studies, can be explained from this structure and is in agreement with the observed decrease in the gel-to-liquid crystalline phase transition temperature of 4 °C for 2-*sn*-DPPC (Seelig et al., 1980).

However, this new configuration of the glycerol backbone has no measurable effect on the phosphorus chemical shift anisotropy of 2-*sn*-DPPC in the fluid phase. This already indicates that the influence of this new configuration on the phosphocholine headgroup conformation should not be considerable. The quadrupole splitting of the α-CD_2 segment in this new compound increased by only 2 kHz and the splitting in the β-CD_2 segment decreased by 0.5 kHz compared to DPPC. The temperature dependence of the order parameters is the same for both molecules.

V. The Final Picture

The investigations now reviewed demonstrate that the complex static and dynamic structure of the various phospholipid head groups in model membranes can be successfully approached by combining

the specific advantages of several methods. It has been shown that some characteristic conformational features, common to the single-crystal structures of DLPE and DMPC, are also maintained for less-ordered membrane phases in an aqueous environment. The liquid crystalline phases of four phospholipids (PC, PE, PG and PS) exhibit the same pattern of quadrupole splittings for the first methylene segment in both chains and this can be attributed to a conformation as already observed in this region for the crystals. Neutron diffraction data have supported this result also for the gel state of PC and PE by determining an axial displacement between corresponding segments in the two fatty acyl chains. All these findings were a first indication for a more general glycerol backbone structure. Additionally, ^2H NMR measurements on the glycerol-C3-segment for different phospholipid compounds confirmed this structure.

For zwitterionic phospholipids, single-crystal data and, for the gel and fluid state, neutron diffraction results showed that the overall orientation defined by the P-N vector is almost parallel to the bilayer surface. To elucidate the internal structural and motional details of head groups in biologically interesting phases, NMR techniques have been the most informative methods used so far. However, the experimental information is as yet not sufficient to provide an adequate description of the behavior of this structural part of the molecule. It is interesting at this point to consider the concepts used to interpret the same kind of data in the chain region. There the symmetry of the problem allowed one to introduce the simple rotational isomeric model in conjunction with reasonable assumptions for the intermolecular interactions. The chemical and structural heterogeneity in the polar region does not permit this approach and insight into the structure of this region must be otherwise obtained. As has been shown in section IV the comparison of various observed data for chemically different head groups can provide some reliable conclusions by purely correlating chemical modifications in the head groups with changes in the measured quantities. A fruitful continuation of this approach will be a systematic chemical modification of a given head group, e.g. by changing the number of donor and acceptor functions for hydrogen bonds and the length or charge of the head group. Another direction for further experiments would be a systematic investigation of the influence of variations in the aqueous environment on the headgroup structure and mobility.

We are sincerely indebted to Dr. U.P. Fringeli from the Swiss Federal Institute of Technology Zürich for expertly describing the infrared spectroscopy method and for his helpful comments; furthermore, to Prof. J. Seelig and Drs. J. Browning, J.P. Meraldi and J.C.W. Shepherd for many valuable and fruitful discussions. This work was supported by grant 3.409.78 from the Swiss National Science Foundation (to G.B.).

References

Abrahamsson, S., Pascher, I. 1966. *Acta Crystallogr.* **21**:79
Akutsu, H., Kyogoku, Y., Nakahara, H., Fukuda, K. 1975. *Chem. Phys. Lipids* **15**:222
Bellamy, L.J. 1975. The Infrared Spectra of Complex Molecules. Methuen & Co., London
Brown, M.F., Seelig, J. 1978. *Biochemistry* **17**:381
Brown, M.F., Seelig, J., Häberlen, U. 1979. *J. Chem. Phys.* **70**:5045
Browning, J., Seelig, J. 1980. *Biochemistry* **19**:1262
Büldt, G., Gally, H.U., Seelig, A., Seelig, J., Zaccai, G. 1978. *Nature* **271**:182
Büldt, G., Gally, H.U., Seelig, J., Zaccai, G. 1979. *J. Mol. Biol.* **134**:673
Büldt, G., Seelig, J. 1980. *Biochemistry (In press)*
Burnett, L.J., Müller, B.H. 1971. *J. Chem. Phys.* **55**:5829
Cullis, P.R., De Kruijff, B. 1979. *Biochim. Biophys. Acta* **559**:399
Davis, J.H. 1979. *Biophys. J.* **27**:339
Davis, J.H., Jeffrey, K.R., Bloom, M., Valic, M.I., Higgs, T.P. 1976. *Chem. Phys. Lett.* **42**:390
Elder, M., Hitchcock, P., Mason, R., Shipley, G.G. 1977. *Proc. R. Soc. London* **A354**:157
Franks, N.P., Lieb, W.R. 1979. *J. Mol. Biol.* **133**:469
Fringeli, U.P. 1977. *Z. Naturforsch.* **32c**:20
Fringeli, U.R. 1980. *Biophys. J. (In press)*
Gally, H.U., Niederberger, W., Seelig, J. 1975. *Biochemistry* **14**:3647
Gally, H.U., Pluschke, G., Overath, P., Seelig, J. 1979. *Biochemistry* **18**:5605
Gally, H.U., Pluschke, G., Overath, P., Seelig, J. 1980. *Biochemistry* **19**:1638
Griffin, R.G., Powers, L., Pershan, P.S. 1978. *Biochemistry* **17**:2718
Haberkorn, R.A., Griffin, R.G., Meadows, M.D., Oldfield, E. 1977. *J. Am. Chem. Soc.* **99**:7353
Harrick, N.J. 1967. Internal Reflection Spectroscopy. J. Wiley & Sons, New York
Hauser, H., Phillips, M.C. 1979. *Prog. Surf. Membr. Sci.* **13**:297
Herzberg, G. 1945. Infrared and Raman Spectra Polyatomic Molecules. Van Nostrand, New York
Herzfeld, J., Griffin, R.G., Haberkorn, R.A. 1978. *Biochemistry* **17**:2711
Hitchcock, P.B., Mason, R., Thomas, R.M., Shipley, G.G. 1974. *Proc. Nat. Acad. Sci. USA* **71**:3036
Kaatze, U., Henze, R., Eibl, H. 1979. *Biophys. Chem.* **10**:351
Kaatze, U., Henze, R., Pottel, R. 1979. *Chem. Phys. Lipids* **25**:149
Kittel, C. 1971. Introduction to Solid State Physics, 4th Edition. John Wiley & Sons, New York
Kleemann, W., McConnell, H.M. 1976. *Biochim. Biophys. Acta* **410**:206
Kohler, S.J., Klein, M.P. 1977. *Biochemistry* **16**:519
Lee, A.G., Birdsall, N.J.M., Metcalfe, J.C., Warren, G.B., Roberts, G.C.K. 1976. *Proc. R. Soc. Lond., B.* **193**:253
Lesslauer, W., Blasie, J.K. 1972. *Biophys. J.* **12**:175
Levine, Y.K., Wilkins, M.H.F. 1971. *Nature New Biol.* **230**:69
Marčelja, S. 1974. *Biochim. Biophys. Acta* **367**:165
Meraldi, J.P., Schlitter, J. 1980. *Biochim. Biophys. Acta (in press)*
Oldfield, E., Meadows, M., Rice, E., Jacobs, R. 1978. *Biochemistry* **17**:2727
Overath, P., Schairer, H.U., Stoffel, W. 1970. *Proc. Nat. Acad. Sci. USA* **67**:606

Pape, E.H. 1974. *Biophys. J.* **14**:284
Pearson, R.H., Pascher, I. 1979. *Nature (London)* **281**:499
Powers, L., Persham, P.S. 1977. *Biophys. J.* **20**:137
Rihak, P. 1979. Raman and Infrarot-Spektroskopie von Cholin und Lezithin. ETH-Thesis Nr. 6393, Zürich
Rouser, G., Nelson, G.J., Fleischer, S., Simon, G. 1968. *In:* Biological Membranes. D. Chapman, editor. Vol. 2, pp. 5-64. Academic Press, New York
Sackmann, E. 1978. *Ber. Bunsenges. Phys. Chem.* **82**:891
Sandermann, H. 1978. *Biochim. Biophys. Acta* **515**:209
Schindler, H., Seelig, J. 1975. *Biochemistry* **14**:2283
Schwartz, S., Cain, J.E., Dratz, E.A., Blasie, J.K. 1975. *Biophys. J.* **15**:1201
Seelig, A., Seelig, J. 1975. *Biochim. Biophys. Acta* **406**:1
Seelig, J. 1977. *Q. Rev. Biophys.* **10**:353
Seelig, J. 1978. *Biochim. Biophys. Acta* **515**:105
Seelig, J., Browning, J. 1978. *FEBS Lett.* **92**:41
Seelig, J., Dijkman, R., de Haas, G.H. 1980. *Biochemistry* **19**:2215
Seelig, J., Gally, H.U. 1976. *Biochemistry* **15**:5199
Seelig, J., Gally, H.U., Wohlgemuth, R. 1977. *Biochim. Biophys. Acta* **467**:109
Shepherd, J.C.W., Büldt, G. 1978. *Biochim. Biophys. Acta* **514**:83
Shepherd, J.C.W., Büldt, G. 1979. *Biochim. Biophys. Acta* **558**:41
Skarjune, R., Oldfield, E. 1980. *Biochemistry* **18**:5903
Stockton, G.W., Polnaszek, C.F., Tulloch, A.P., Hasan, F., Smith, I.C.P. 1976. *Biochemistry* **15**:954
Sundaralingam, M. 1972. *Ann. N.Y. Acad. Sci. USA* **195**:324
Träuble, H., Eibl, H. 1974. *Proc. Nat. Acad. Sci. USA* **71**:214
Wilson, E.B., Decius, J.C., Cross, P.C. 1955. Molecular Vibrations. McGraw Hill Book Company, New York
Wohlgemuth, R., Waespe-Šarčevic, N., Seelig, J. 1980. *Biochemistry* **19**:3315
Worcester, D.L., Franks, N.P. 1976. *J. Mol. Biol.* **100**:359
Worthington, G.R., King, G.I., McIntosh, T.J. 1973. *Biophys. J.* **13**:480
Yeagle, P.L. 1978. *Accounts Chem. Res.* **11**:321
Yeagle, P.L., Hutton, W.C., Huang, C., Martin, R.B. 1975. *Proc. Nat. Acad. Sci. USA* **72**:3477
Yeagle, P.L., Hutton, W.C., Huang, C., Martin, R.B. 1976. *Biochemistry* **15**:2121
Zaccai, G., Blasie, J.K., Schoenborn, B.P. 1975. *Proc. Nat. Acad. Sci. U.S.A.* **72**:376
Zaccai, G., Büldt, G., Seelig, A., Seelig, J. 1979. *J. Mol. Biol.* **134**:693

Received 3 March 1980; revised 16 July 1980